To be presented at the 32nd ILRC in Hiroshima, Japan, 5-10 July 2026.

Near-surface multiscale turbulent coherent structures observed by the REAL at M²HATS

Shane D. Mayor and Pierre Dérian
California State University Chico
Dept. of Earth and Environmental Sciences, 400 West First St., Chico, CA, 95929-0205, USA
Lead Author e-mail address: sdmayor@csuchico.edu

Abstract: We describe moving patches of aerosol streaks observed by horizontal scans of the REAL from the 2023 M²HATS in Tonopah, Nevada. The features occur on windy, unstable afternoons with deep convective boundary layers. We focus on a single example observed on 18 August 2023, at approximately 21:18 UTC, in which a crescent-shaped patch passed directly over a horizontal linear array of fast-response sensors. As the feature passed, wind speed and temperature increased. Our current working hypothesis is that the patch results from a large-eddy-scale downdraft and that the streaks within the patch result from increased near-surface wind speed that lifted particulate matter from the surface and advected it into convergence bands.

1. Introduction

Large, on the order of 1 km, patches of finely structured aerosol backscatter that move downstream in the direction of the mean flow are consistently observed in horizontal scans from the Raman-shifted Eye-safe Aerosol Lidar (REAL)[1] during windy and convective conditions in the 2023 Multipoint MOST Horizontal Array Turbulence Study (M²HATS) [2]. The REAL was scanned horizontally for approximately 60 days, from 23 July to 25 September 2023, to observe the 2D, 2-component horizontal vector wind field [3]. These data will be used to test multipoint Monin-Obukhov Similarity Theory (MOST) [4]. The experimental site is a high-altitude (1655 m ASL) desert environment in a broad (order 10 km) and nearly flat valley, less than 1 km south of the 15/33 runway at Tonopah Airport (TPH).

The broad patches contain fine-scale (order 10 – 100 m), wind-parallel, streak-like structures. The patches often exhibit an asymmetric structure in the streamwise direction. They evolve rapidly in time as they move, and sometimes they appear and disappear. They frequently have a catspaw-like appearance. The dataset contains hundreds, perhaps thousands, of such events or features. Here, we focus on the afternoon of 18 August 2023, when one particularly crescent-shaped feature (see Fig. 1) moved over the National Center for Atmospheric Research (NCAR) Integrated Surface Flux System (ISFS) linear array. Our long-term goals are to identify and name the features, understand the dynamics that drive them, and determine how they contribute to turbulent transport.

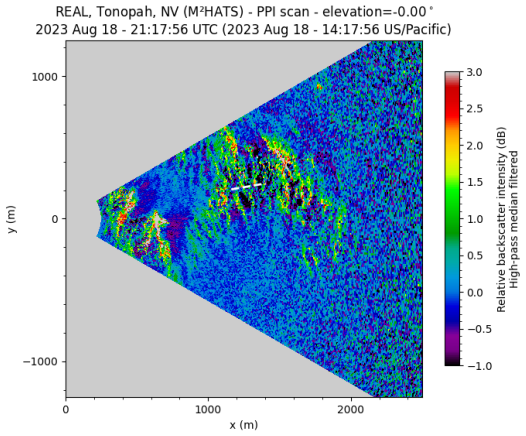

Figure 1. A single high-pass median filtered scan of relative aerosol backscatter from the REAL, acquired when the aerosol patch was located over the 245 m wide linear array (white dashed line).

2. Weather discussion

Upper-air conditions on 18 August 2023 were characterized by weak large-scale forcing over western Nevada. At 500 mb, geopotential heights in the Tonopah region were approximately 586.5 dam, inferred from analyzed height contours and surrounding station values. The site lay on the northwestern periphery of a broad mid-tropospheric ridge

centered over the southern Plains, within modest south-to-southwesterly flow and weak horizontal height gradients. The curvature and gradients over central Nevada were weak, implying minimal synoptic-scale vertical motion. Under these conditions, boundary-layer processes and mesoscale circulations dominated the near-surface structure during the period of interest.

Visible satellite imagery indicates a generally cloud-free environment over the M^{2}HATS site during the analysis period of 18 August, with scattered afternoon convection confined to the surrounding higher terrain. No organized synoptic cloud systems or frontal features were present in the region. These conditions are consistent with strong surface heating and an active convective boundary layer, suggesting that local and mesoscale processes dominate the near-surface variability at the site.

Near-surface meteorological conditions on 18 August exhibited a pronounced diurnal cycle characteristic of a dry, strongly heated valley environment. Air temperature reached a morning minimum of approximately 14–16°C and increased steadily throughout the day, attaining afternoon and early evening values of approximately 30–31 °C during the period of interest. Dew point remained low throughout the day, generally between −6 and 0 °C, indicating persistently dry conditions and a large daytime dew-point depression. Surface pressure varied smoothly over the diurnal cycle, consistent with thermally driven boundary-layer evolution rather than synoptic forcing. Wind speeds were weak during the night and early morning (~1–3 m s^{-1}) with predominantly northerly flow, and increased substantially during the daytime (~5–10 m s^{-1}) as winds shifted to southerly flow, consistent with the development of a thermally driven up-valley circulation in the north–south-oriented Rawlins Valley, as documented during M^{2}HATS.

3. Boundary Layer Heights

The afternoon boundary layer at the M^{2}HATS site on 18 August 2023 was deep and convective, as indicated consistently by multiple independent observing systems [5]. A radiosonde launched at 21:57:53 UTC showed a well-mixed virtual potential temperature profile up to approximately 3.5 km AGL, above which θ_v increased rapidly, marking the transition to a stable free atmosphere. Vertical-stare aerosol backscatter from the NCAR MicroPulse DIAL (MPD) exhibited an elevated aerosol layer capped near 3–4 km AGL, with algorithm-derived boundary-layer height estimates tracking the aerosol-layer top and remaining below cloud bases. Radar wind profilers operating at 915 and 449 MHz independently showed enhanced reflectivity below a coherent upper boundary that rose through the afternoon, with boundary-layer height estimates reaching approximately 3.5–4 km AGL by late afternoon to early evening. Consistent with these measurements, Doppler-lidar observations of vertical-velocity variance showed a daytime turbulent layer capped by boundary-layer height estimates at similar altitudes. A brief period of boundary-layer clouds occurred earlier in the day (approximately 14–15 local time), well before the late-afternoon interval analyzed here.

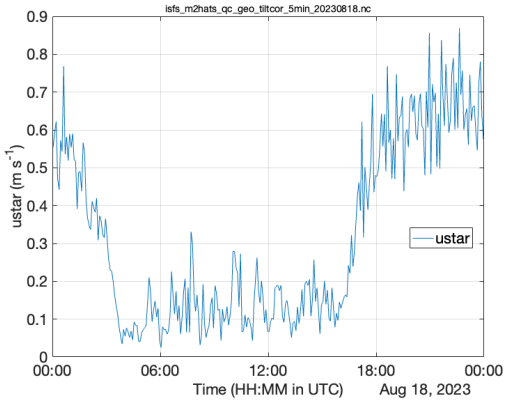

Figure 2. Friction velocity u_* from the NCAR ISFS linear array (tower 26), shown as 5-min averages for 18 August 2023.

4. Surface fluxes

Surface-layer forcing on 18 August 2023 was characterized by both strong mechanical stress and strong thermal buoyancy. Five-minute ISFS measurements at tower 26 (4 m AGL), located near the center of the linear array, show friction velocity u_* increasing from weak nocturnal values ($\sim 0.05 - 0.15$ m s^{-1}) to sustained afternoon values of approximately 0.5–0.8 m s^{-1}, indicating vigorous surface stress and strong coupling between the surface and the convective boundary layer. Sensible heat flux became strongly positive during the afternoon, reaching peak kinematic values of roughly 0.4–0.55 m s^{-1} °C, while moisture flux remained near zero throughout the day. The surface energy balance was therefore strongly

dominated by sensible heat flux, consistent with dry surface conditions and a large Bowen ratio.

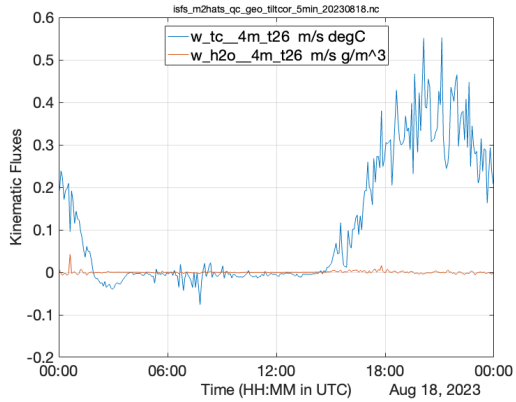

Figure 3. 5-minute averages of the surface sensible and latent heat fluxes for 18 August.

5. Structures in the REAL images

The sequence of scan images collected by the REAL every 17 s reveals recurrent, spatially coherent regions of enhanced backscatter variability embedded within a weaker, more homogeneous aerosol-scattering background. Figures 1 and 4 show a crescent-shaped patch as it passed over the 245 m wide linear array. Figure 4 has undergone Sasano image distortion correction [6] to account for the time required to scan the sector, while aerosol features continue to advect with the mean flow. The crescent is about 1 km wide in the east-west dimension by about 500 m long in the north-south dimension. The wind-parallel aerosol streaks have an order-of-magnitude spacing of 100 m and taper into the background at both ends. The streaks are irregular, intermittently merging and terminating, and exhibit stronger contrast within the patch than in the surrounding background. Both the patch-scale structures and their internal substructure evolve smoothly and are advected coherently across the scan domain, persisting over tens of seconds. The observed phenomenon is intermittent but recurring, suggesting that this case is representative of a broader class of similar events present throughout the dataset.

Figure 5 shows the horizontal vector motion field that was derived from two consecutive pairs of scans using the Typhoon wavelet-based motion estimation algorithm [3]. It confirms prevailing southerly flow, convergence north of the crescent, and weak divergence south of the crescent.

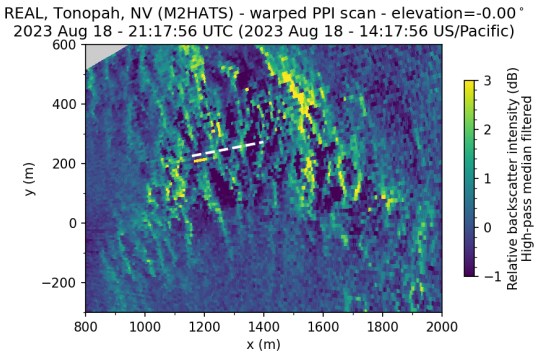

Figure 4. Zoomed-in version of Fig. 1 with a different color bar and the Sasano [6] image distortion correction applied to better show the streaky structures in the aerosol patch. The streaks tend to be wind parallel but do merge in some locations.

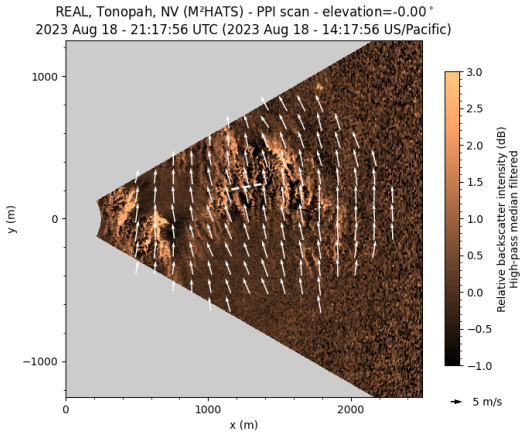

Figure 5. Derived vector flow field superimposed on high-pass median filtered aerosol backscatter.

6. Linking lidar to in situ data

Scalars organize on velocity structures, and the surface of this dry environment is a source of particulate matter. To link the lidar images to the in situ data, we calculated the variance of the high-pass, median-filtered aerosol backscatter pixels in a line segment that was close to and colinear with the linear array. The aerosol backscatter variance is larger inside the patches. Figure 6 shows the variance as a function of time. Each point on the graph represents the variance from a single scan. It shows the variance spiking as the patch first moves over the array shortly after 21:16 UTC, with 2 or 3 subsequent local maxima, and then returning to low variance after the patch moves away at 21:20 UTC.

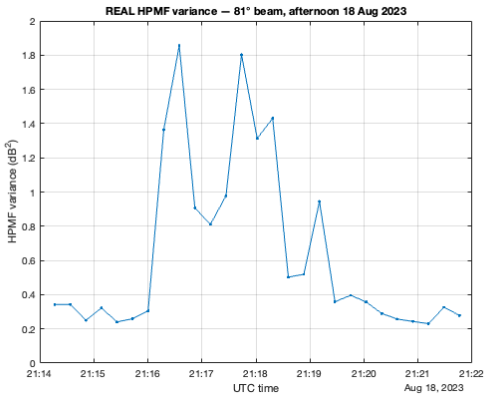

Figure 6. Variance of filtered aerosol backscatter from the REAL versus time for the radial row of pixels near the linear array over time.

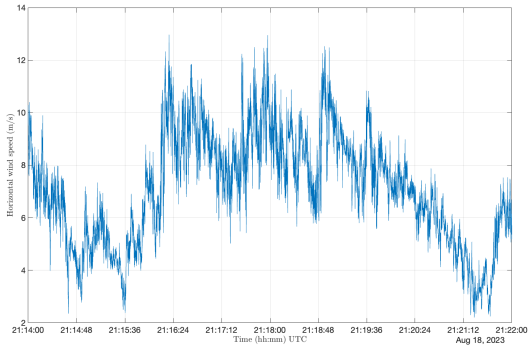

Figure 7. Horizontal wind speed at 4 m AGL from tower number 26 in the linear array.

7. Linear array data

The linear array consisted of 50 sonic anemometers spaced 5 m apart at 4 m AGL. The row orientation was perpendicular to the mean flow direction. Tower number 26 was approximately in the middle of the array. The wind-speed time series (Figure 7) shows a three-pronged maximum that temporally aligns with a similar three-pronged set of maxima in the HPMF variance time series shown in Figure 6. The three gusts exceed 12 m s^{-1} (27 mph). Wind speed traces from other towers show a similar shape. Over the same time interval, the mean vertical velocity at 4 m AGL is negative at most array locations, indicating persistent near-surface subsidence across the 245 m cross-stream extent of the array. Because the in situ sensors sample only the surface layer, the observed subsidence is interpreted as the near-surface expression of larger-scale descending motion rather than a direct observation of a large-eddy downdraft. Air temperature increased by about 0.5°C as the patch moved over.

8. Conclusions

This work was performed under NSF Award number 2054969. We plan to continue examining the in situ data from this case study and to process the entire M^2HATS dataset to better characterize these patches and assess their implications for near-surface turbulent transport.

9. References

[1] S. D. Mayor, S. M. Spuler, B. M. Morley, and E. Loew, "Polarization lidar at 1.54 microns and observations of plumes from aerosol generators," Opt. Eng. 46, 096201 (2007).

[2] C. Tong et al., "Multipoint Monin-Obukhov Similarity Theory Horizontal Array Turbulence Study (M^2HATS)," Bull. Amer. Meteor. Soc., Accepted (2026).

[3] P. Dérian, C. F. Mauzey, and S. D. Mayor, "Wavelet-based optical flow for two-component wind field estimation from single aerosol lidar data," J. Atmos. Oceanic Technol. 32, 1759–1778 (2015).

[4] M. Ding and C. Tong, "Multi-Point Monin–Obukhov similarity of turbulence cospectra in the convective atmospheric boundary layer," Boundary-Layer Meteorol. 178, 185–199 (2021).

[5] C. P. Young, L. Colberg, W. Brown, S. M. Spuler, K. Repasky, C. Tong, and S. D. Mayor, "Daytime boundary layer heights at Tonopah, Nevada, from M^2HATS," presented at the 25th Symposium on Boundary Layers and Turbulence, American Meteorological Society, Torino, Italy, 17–20 June (2025).

[6] Y. Sasano, H. Hirohara, T. Yamasaki, H. Shimizu, N. Takeuchi, and T. Kawamura, "Horizontal wind vector determination from the displacement of aerosol distribution patterns observed by a scanning lidar," *J. Appl. Meteor.* **21**, 1516–1523 (1982).